Electron–LO-phonon scattering rates in a cylindrical quantum wire with an axial magnetic field: Analytic results

M. Masale and N. C. Constantinou*
Department of Physics, University of Essex, Colchester CO4 3SQ, England
(Received 5 April 1993)

The interaction of electrons with bulk LO phonons in a cylindrical quantum wire is discussed with both intersubband and intrasubband relaxation considered. For processes involving the lowest pair of subbands, a parallel analytic approach leads to good agreement with the numerical calculations. In particular, the effect of an axial magnetic field is determined for intersubband transitions between these two subbands. It is found that for a given radius, there is a critical magnetic field beyond which first-order LO-phonon interactions are forbidden due to energy conservation. Close to the critical fields, fast intersubband relaxation is predicted. These effects are a consequence of the Zeeman splitting of the doubly degenerate states in the presence of the field and the behavior of the one-dimensional density of states.

I. INTRODUCTION

The recent advent of growth techniques which allow carriers to be confined in two spatial dimensions resulting in quasi-one-dimensional (Q1D) behavior has led to a great deal of interest, both experimental[1–5] and theoretical.[6–13] In particular, the realization of the extreme quantum limit by Plaut *et al.*[5] is an important step towards the goal of high-mobility devices which depend on the reduced phase space to suppress elastic scattering at low temperatures.[6] At higher temperatures the dominant scattering mechanism is via LO phonons. The interaction of electrons with LO phonons in Q1D systems has been treated theoretically by a number of people. Leburton[8] considered the electron–LO-phonon interactions in rectangular wires as did Campos and Das Sarma.[9] Constantinou and Ridley[10] investigated intrasubband scattering in cylindrical wires and this was recently extended by Leao, Hipolito, and Peeters[11] to take into account many subbands. All of these studies have been essentially numerical in nature. Fishman[12] has presented analytic results for the electron-phonon–scattering rates in the extreme quantum limit for cylindrical wires by assuming a constant ground-state radial wave function.

Recently, Gold and Ghazali[13] have introduced approximate wave functions for the first two subbands of a cylindrical wire in order to determine analytically various physically interesting properties of cylindrical wires, such as the low-temperature mobility and the plasmon spectrum among other things. The advantages of having analytic expressions which reproduce, to a good approximation, the exact results is not only in the saving of computational time which they facilitate, but they also make the physics rather more transparent. In this paper, the scattering rates for the interaction of electrons are derived for an arbitrary number of subbands of a cylindrical quantum wire. For intrasubband scattering within the ground state and intersubband scattering between the first excited state and the ground state, analytic expressions for the scattering rates are determined by employing the approximate wave functions of Gold and Ghazali and these rates are then compared to the numerical results. Furthermore, the effect of an applied axial magnetic field on the intersubband rates is readily incorporated within this analytic scheme.

The paper is organized as follows. Section II develops the formalism for determining the scattering rates between any pair of electron levels. Section III applies this to intrasubband and intersubband relaxation both numerically, by employing the exact wave functions, and analytically by using the approximate wave functions of Gold and Ghazali. Section IV contains our conclusions.

II. FORMALISM

We consider a cylindrical wire of length L_z (assumed to be effectively infinite) and radius R. The assumption of a cylindrical quantum wire is not only convenient from the mathematical point of view, but also has practical relevance as Tonucci *et al.*[14] have recently successfully fabricated cylindrical wires with diameters as small as 330 Å. Cylindrical wires have also recently been considered in related areas, with Branis, Li, and Bajaj[15] investigating the effect of an applied axial magnetic field on hydrogenic impurities, and Ihm *et al.*[16] the magnetization.

The carriers are assumed to be confined by an infinite potential, and from symmetry the solutions to the one-electron effective-mass equation with parabolic bands is separable even in the presence of an axial magnetic field,[17,18] and may be written down in cylindrical coordinates (r,ϕ,z) as

$$\Psi_{mnk}(r,\phi,z)=\frac{1}{V^{1/2}}e^{im\phi}e^{ikz}\psi_{mn}(r)\ , \quad r<R$$

$$m=0,\pm1,\pm2,\pm3\ldots\ , \qquad (1)$$

where $V=(\pi R^2 L_z)$ is the volume of the wire, $\psi_{mn}(r)$ is the radial wave function, m is the azimuthal quantum number, n is the radial quantum number $(n=1,2,3\ldots)$, and k is the axial wave vector. For the moment we keep the form of the radial wave function general. The energy of the electron E is simply given by

$$E(m,n,k)=E_{mn}(B)+E_k \; , \tag{2}$$

where $E_{mn}(B)$ is the subband energy, which will be dependent on the applied axial magnetic field B and is determined by requiring the radial wave function to vanish at $r=R$. For convenience we label the subbands by their m and n quantum numbers (m,n), E_k is the energy in the axial direction which is given by the familiar parabolic form

$$E_k=\hbar^2k^2/2m^* \tag{3}$$

with m^* the electronic effective mass ($=0.067m_e$ for GaAs). In what follows we assume that electrons scatter from a state $|mnk\rangle$ to another state $|m'n'k'\rangle$ via the interaction with bulk LO phonons. There are theoretical reasons[19,20] that such an approximation for the phonons holds well for the analogous two-dimensional GaAs/AlAs system, and as such we ignore the effects of the boundaries on the LO-phonon spectrum.

The Fröhlich interaction Hamiltonian is given by[21]

$$H_{\text{int}}=\sum_q C(q)\{ae^{i\mathbf{q}\cdot\mathbf{R}}+a^+e^{-i\mathbf{q}\cdot\mathbf{R}}\} \tag{4}$$

with the coupling factor expressed as

$$C(q)=\frac{i}{q}\left[\frac{e^2\hbar\omega_L}{2\varepsilon_0 V_c}\left[\frac{1}{\varepsilon_\infty}-\frac{1}{\varepsilon_s}\right]\right]^{1/2} . \tag{5}$$

In the above, ε_0 is the permittivity of free space, ε_∞ ($=10.9$) and ε_s ($=13.1$) are the high- and low-frequency dielectric constants, ω_L ($=36.6$ meV) is the LO-phonon zone-center frequency, V_c is the volume of the crystal, and the values quoted are those appropriate for GaAs. As we are only concerned with bulk three-dimensional phonons, their total wave vector q in the cylindrical system is simply

$$q=(q_r^2+q_z^2)^{1/2} \; , \quad 0\le q_r<\infty \; , \quad -\infty<q_z<\infty \tag{6}$$

with q_r the radial component of the wave vector and q_z the axial component.

We are now in a position to evaluate the matrix elements for scattering from an initial combined electronic and phonon state $|i\rangle$ to that of the final state $|f\rangle$, viz.,

$$M^{\overset{e}{a}}=\langle i|H_{\text{int}}|f\rangle=2C(q)[N(\omega_L)+\tfrac{1}{2}\pm\tfrac{1}{2}]^{1/2} \times e^{-i(m-m')\pi/2}I_{mnm'n'}(y)\delta_{k'-k\pm q_z,0} \; . \tag{7}$$

In the above, $N(\omega_L)$ is the Bose-Einstein distribution, e and a refer to the emission or absorption of a phonon, and the δ function conserves the axial momentum. The scattering integral $I_{mnm'n'}(y)$ is given by

$$I_{mnm'n'}(y)=\int_0^1 xJ_{|m-m'|}(yx)\psi^*_{m'n'}(x)\psi_{mn}(x)dx \; , \tag{8}$$

where $x=r/R$ and $y=q_rR$.

The scattering rate is evaluated via Fermi's golden rule

$$\Gamma^{\overset{e}{a}}=\frac{2\pi}{\hbar}\sum_q|M^{\overset{e}{a}}|^2\delta[E(m,n,k)-E(m',n',k')\mp\hbar\omega_L] \tag{9}$$

which after transforming the summation over the wave vector to an integration leads finally to the following general result for the emission or absorption rate from state $|mnk\rangle$ to state $|m'n'k'\rangle$:

$$\Gamma^{\overset{e}{a}}=2\Gamma_0[N(\omega_L)+\tfrac{1}{2}\pm\tfrac{1}{2}]\{\varepsilon_i\mp(1-\Delta\varepsilon)\}^{-1/2}\int_0^\infty H(y)dy \; , \tag{10}$$

where $H(y)$ is given by

$$H(y)=y|I_{mnm'n'}(y)|^2\left[\frac{1}{y^2+Q_{\alpha+}^2}+\frac{1}{y^2+Q_{\alpha-}^2}\right] , \quad \alpha=e,a \tag{11}$$

and the scaled energies are

$$\varepsilon_i=\frac{E_k}{\hbar\omega_L} \tag{12}$$

and

$$\Delta\varepsilon=\frac{|E_{mn}(B)-E_{m'n'}(B)|}{\hbar\omega_L} \; . \tag{13}$$

The scaled axial phonon wave vectors are given by

$$Q_{e\pm}=Q_0(\sqrt{\varepsilon_i}\mp\{\varepsilon_i-1+\Delta\varepsilon\}^{1/2}) \; , \tag{14}$$

$$Q_{a\pm}=Q_0(-\sqrt{\varepsilon_i}\pm\{\varepsilon_i+1-\Delta\varepsilon\}^{1/2}) \; , \tag{15}$$

with $Q_0=(2m^*\omega_LR^2/\hbar)^{1/2}$, and in Eqs. (14) and (15) the $+$ and $-$ subscripts on the wave vectors refer to forward and backward scattering. Finally, Γ_0 is given by

$$\Gamma_0=2\alpha\omega_L=\frac{e^2}{4\pi\varepsilon_0\hbar}\left[\frac{1}{\varepsilon_\infty}-\frac{1}{\varepsilon_s}\right]\left[\frac{2m^*\omega_L}{\hbar}\right]^{1/2} , \tag{16}$$

where α is the dimensionless Fröhlich coupling constant[21] ($\Gamma_0\approx 8.7\times10^{12}$ s^{-1} for GaAs).

Equation (10) represents the general expression for the scattering rate from state $|mnk\rangle$ to state $|m'n'k'\rangle$ by the emission or absorption of an LO phonon. It agrees with previous investigations for a cylindrical wire[10,11] and as is seen involves two integrations which in general have to be evaluated numerically. In the following section specific applications are made.

III. APPLICATIONS

Case (i). Zero magnetic field. We first consider scattering in the absence of a magnetic field which has been dealt with previously in the extreme quantum limit by Constantinou and Ridley[10] and more generally for many-subband relaxation by Leao, Hipolito, and Peeters.[11] The radial solutions to the effective-mass Schrödinger equation are Bessel functions (the definitions of all the special functions employed in this paper may be found in Ref. 22), viz.,

$$\psi_{mn}(x)=\frac{1}{J_{m+1}(j_{mn})}J_m(j_{mn}x) \tag{17}$$

with the corresponding subband energy

$$E_{mn}(0)=\frac{\hbar^2}{2m^*}\left[\frac{j_{mn}}{R}\right]^2 . \tag{18}$$

In Eq. (18) j_{mn} is the nth zero of $J_m(z)$, ($j_{01}=2.405$ and $j_{11}=3.832$). The integration involved in Eq. (8) has, to our knowledge, no analytic form, and by implication the integrals of (8) and (11) need to be evaluated numerically. This has been carried out in a recent investigation.[11] Here, we derive an analytic expression for the intrasubband rate involving transitions within the lowest subband (0,1), and the intersubband scattering rate between the first excited state and (0,1). These transitions are important in the analogous Q2D system and significant experimental investigations have been carried out in 2D to investigate intrasubband relaxation by Tsen *et al.*[23] and intersubband relaxation by Tatham, Ryan, and Foxon[24] and Grahn *et al.*[25] More recently, Mayer *et al.*[26] have investigated energy relaxation in quantum wires and Oowaki *et al.*[27] have reported enhanced intersubband relaxation in a one-dimensional constriction. As such, reliable analytic results for scattering rates are both useful and instructive, and it should be emphasized that early investigations on the electron-phonon interactions in quasi-two-dimensional systems, such as the investigations by Price[28] and Ridley,[29] also endeavored to develop corresponding analytic approximations to the rates.

We make use of the radial wave functions for the ground state and first excited state employed recently by Gold and Ghazali,[13]

$$\psi_{01}(x)=\sqrt{3}(1-x^2) , \tag{19}$$

$$E_{01}(0)=\frac{6\hbar^2}{2m^*R^2} , \tag{20}$$

$$\psi_{\pm 11}(x)=\sqrt{12}(x-x^3) , \tag{21}$$

$$E_{11}(0)=\frac{16\hbar^2}{2m^*R^2} . \tag{22}$$

Figure 1 compares these approximate wave functions with the exact wave functions given by Eqs. (17) and (18). In these figures the exact wave functions for a radius of 150 Å and applied magnetic field of 15 T are also depicted (see the discussion below).

With the above approximate wave functions, the integrations of Eq. (8) are given in closed form by

$$I_{0101}(y)=24\frac{J_3(y)}{y^3} , \tag{23}$$

$$I_{\pm 1101}(y)=48\frac{J_4(y)}{y^3} . \tag{24}$$

A comparison of the scattering integrals of Eqs. (23) and (24) and their exact counterparts evaluated numerically from Eq. (8) is illustrated in Fig. 2. The agreement between the approximate and exact expressions is very good especially for small radial wave vectors ($y=q_rR$) which

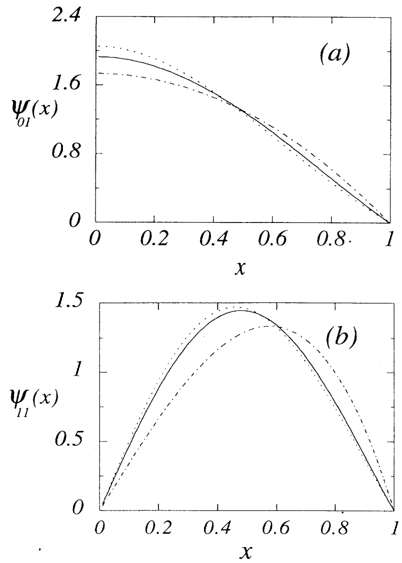

FIG. 1. (a) The (0,1) radial wave function $\psi_{01}(x)$ and (b) the (1,1) wave function $\psi_{11}(x)$. The solid curves depict the Bessel functions given by Eq. (17), the dot-dashed curves are their approximations given by Eqs. (19) and (21), and the dotted curves represent the confluent hypergeometric functions given by Eq. (31) with $R=150$ Å and $B=15$ T.

are just those that are favored by the Fröhlich interaction. Furthermore, the figures illustrate that for intrasubband scattering the favored phonons are those traveling along the axis of the wire, while for intersubband scattering between ($\pm1,1$) and (0,1) it is off-axial phonons that are favored; in fact they are emitted predominantly at right angles to the wire axis when the subband separation is close to $\hbar\omega_L$ ($q_z \ll q_r$).

Substitution of Eqs. (23) and (24) and making use of the infinite integrals evaluated analytically in the Appendix leads to the following expression for the emission and absorption rates:

$$\Gamma^e(\varepsilon_i)=1152\Gamma_0[N(\omega_L)+1]\left[\frac{W_3(Q_{e+})+W_3(Q_{e-})}{\sqrt{(\varepsilon_i-1)}}\right] , \tag{25}$$

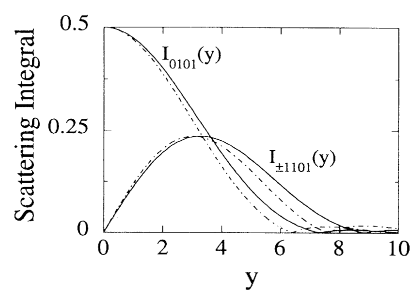

FIG. 2. The scattering integrals as a function of reduced radial phonon wave vector $y(=q_rR)$ with the solid curves representing the exact results and the dot-dashed curves their approximations.

$$\Gamma^a(\varepsilon_i)=1152\Gamma_0 N(\omega_L)\left[\frac{W_3(Q_{a+})+W_3(Q_{a-})}{\sqrt{(\varepsilon_i+1)}}\right], \tag{26}$$

where $W_3(Q)$ is given by (see the Appendix)

$$W_3(Q)=\frac{1}{Q^6}\left\{\frac{1}{6}-\frac{Q^2}{96}+\frac{Q^4}{640}-I_3(Q)K_3(Q)\right\}, \tag{27}$$

where $I_n(z)$ and $K_n(z)$ are modified Bessel functions.[22] Figure 3(a) illustrates the room-temperature ($T=300$ K) emission rate as a function of reduced axial energy calculated with the exact result of Eq. (10) and the approximate analytic result given by Eq. (25) for scattering within the first subband (0,1). The comparison is seen to be excellent for all the energies of interest. The singularity at $\varepsilon_i=1$ is due to the singular nature of the 1D density of states. Of course, in real systems this singularity is smoothed out due to, for instance, geometrical fluctuations. Nevertheless, strong relaxation is predicted near this threshold energy. Figure 3(b) compares the analogous room-temperature absorption rates, and again we find excellent agreement between the two approaches. In both 3(a) and 3(b) the corresponding bulk rates[21] are illustrated for comparison.

We now consider intersubband scattering from the first excited subband (1,1) to the ground state (0,1). We assume that the electron is initially at the bottom of the subband ($\varepsilon_i=0$) and that the temperature is low ($N\approx 0$). The emission rate obtained by employing the Gold and Ghazali wave functions is given by the following expression:

$$\Gamma^e=(96)^2\Gamma_0\left[\frac{W_4(Q_{e+})}{\sqrt{(\Delta\varepsilon-1)}}\right], \tag{28}$$

where $W_4(Q)$ is (see the Appendix)

$$W_4(Q)=\frac{1}{Q^6}\left\{\frac{1}{8}-\frac{Q^2}{240}+\frac{Q^4}{3840}-I_4(Q)K_4(Q)\right\}. \tag{29}$$

Figure 4 depicts the intersubband emission rate as a function of the wire radius R. Again, the agreement between the above analytic expression and the numerical result is very good except close to the critical radius. This critical radius beyond which first-order intersubband transitions are forbidden is given by

$$E_{11}(0)-E_{01}(0)=\hbar\omega_L \tag{30}$$

and will be different for the exact and approximate results due to the slight differences in the subband separation. If the exact subband separation is employed in Eq. (28), the agreement with the numerical result is very good throughout the entire range of radii as is shown in the diagram.

Case (ii). Applied axial magnetic field. The effective-mass equation with an axial magnetic field B is exactly solvable in terms of the confluent hypergeometric function $M(a,b,\xi)$, and the details are discussed in the work of Constantinou, Masale, and Tilley[17] and are not repeated here for brevity. The solution is given by

$$\psi_{mn}(x)=A_{mn}\exp\left[-\frac{\xi}{2}\right]\xi^{|m|/2}M(a_{mn},b,\xi), \tag{31}$$

where ξ is dimensionless and is related to the cyclotron radius R_c via

$$\xi=\frac{x^2R^2}{2R_c^2}. \tag{32}$$

The b parameter is

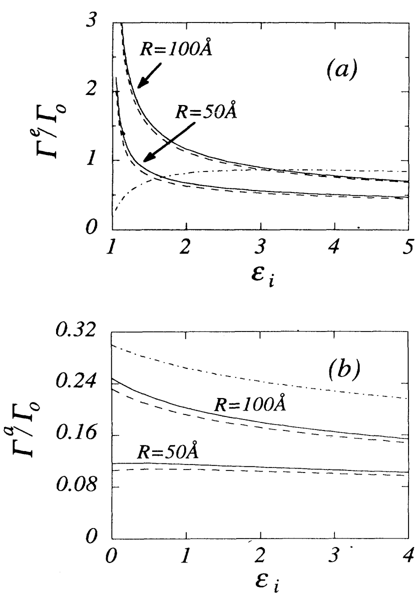

FIG. 3. The room-temperature intrasubband emission rates (a) and absorption rates (b) as a function of the electron's initial axial energy for two different radii. The full curves are the exact results and the dashed curves their analytic approximations. For a comparison the corresponding bulk rates (Ref. 21)

$$\Gamma^e=\Gamma_0[N(\omega_L)+1]\frac{\sinh^{-1}[\sqrt{(\varepsilon_i-1)}]}{\sqrt{\varepsilon_i}}$$

and

$$\Gamma^a=\Gamma_0 N(\omega_L)\frac{\sinh^{-1}(\sqrt{\varepsilon_i})}{\sqrt{\varepsilon_i}}$$

are shown as the dot-dashed curves.

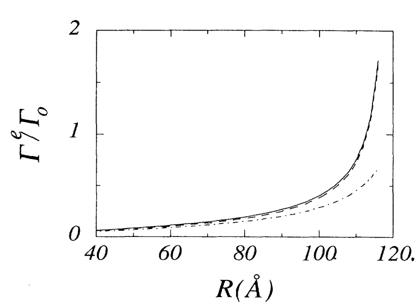

FIG. 4. The intersubband scattering rate as a function of wire radius ($\varepsilon_i=0$). The full curve is the exact result and the dot-dashed curve the analytic approximation. Better agreement is obtained if the same energy separation is used (dashed curve).

$$b=|m|+1 \tag{33}$$

and the parameter a_{mn} is related to the subband energy via

$$E_{mn}(B)=\hbar\omega_c\left[-a_{mn}+\frac{m}{2}+\frac{1}{2}+\frac{|m|}{2}\right] \tag{34}$$

[i.e., a_{mn} is the nth zero of $M(a,b,\xi)$ at $x=1$]. The normalization factor A_{mn} is given by

$$A_{mn}^2=\frac{1}{2\int_0^1 x\psi_{mn}^2(x)dx}\ . \tag{35}$$

The cyclotron radius R_c and the cyclotron frequency ω_c are defined in the usual manner,

$$R_c^2=\frac{\hbar}{eB}\ ,\quad \omega_c=\frac{eB}{m^*}\ . \tag{36}$$

In Figs. 1(a) and 1(b), the radial wave function given by (31) is depicted for the (0,1) and (1,1) subbands for a wire radius of 100 Å and an in-plane magnetic field of 15 T. The difference between this wave function and that obtained using the Bessel functions or the approximate results due to Gold and Ghazali are not too great due primarily to the small wire radius. As we have seen in the previous discussion, intersubband events from the first excited state to the ground state occur for radii less than about 125 Å. The energy of the subbands can be determined from finding the zeros of the confluent hypergeometric function, but for radii of order 150 Å or less and magnetic fields up to 20 T perturbation theory as developed by Dingle[30] is more than adequate, with the subband energies given to an excellent approximation by (see Dingle's paper for the details of the derivation)

$$E_{mn}(B)=E_{mn}(0)+\tfrac{1}{2}m\hbar\omega_c+\tfrac{1}{24}\hbar\omega_c\left[\frac{R^2}{R_c^2}\right]\left\{1+\frac{2(m^2-1)}{j_{mn}^2}\right\},\quad m=0,\pm1,\pm2,\pm3\ldots \tag{37}$$

In what follows the slight difference between the approximate and exact subband energies in the presence of the magnetic field is ignored and Eq. (37) is employed together with Eq. (28). The energy spectrum of a 100-Å quantum wire as a function of applied axial magnetic field is illustrated in Fig. 5. The magnetic field has only a marginal (diamagnetic) effect on the ground state for the system considered in Fig. 5, and as such we do not consider intrasubband relaxation within this band in the presence of a magnetic field. The degeneracy of the $m\neq0$ states is lifted by the presence of the magnetic field and we obtain the Zeeman split states. In particular, the first excited state is $(-1,1)$ which decreases in energy for the magnetic-field strengths shown. It so happens that for this wire radius, the zero-field splitting *is greater than* $\hbar\omega_L$ and as such there will be a critical magnetic field beyond which first-order processes are forbidden. This field is given by the relation

$$E_{-11}(B)-E_{01}(B)=\hbar\omega_L \tag{38}$$

and for a wire of 100 Å this field is around 16 T. For a wire radius of 120 Å, on the other hand, the zero-field splitting between the ground state and the first excited state *is less than* $\hbar\omega_L$, and as such first-order intersubband transitions between $(-1,1)$ and (0,1) are not allowed (for the fields of interest) and hence we consider first-order intersubband transitions between (1,1) and (1,0). This transition is allowed provided the magnetic field is *greater than* a critical value given by

$$E_{11}(B)-E_{10}(B)=\hbar\omega_L \tag{39}$$

which for a wire of radius 120 Å is close to 1 T. This critical field can be further reduced by a decrease in the wire radius. There is yet another critical field which occurs when the cyclotron energy equals the phonon energy

$$E_{11}(B)-E_{-11}(B)=\hbar\omega_L \tag{40}$$

but this field is large and is not considered further. Figure 6(a) illustrates the intersubband scattering rate be-

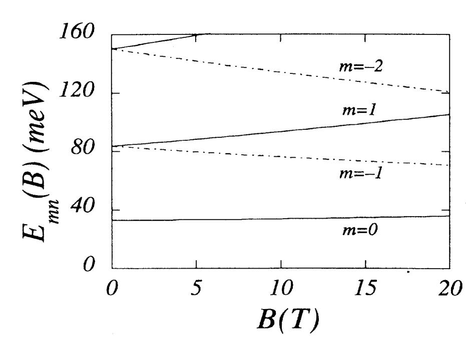

FIG. 5. The subband energies as a function of axial magnetic field.

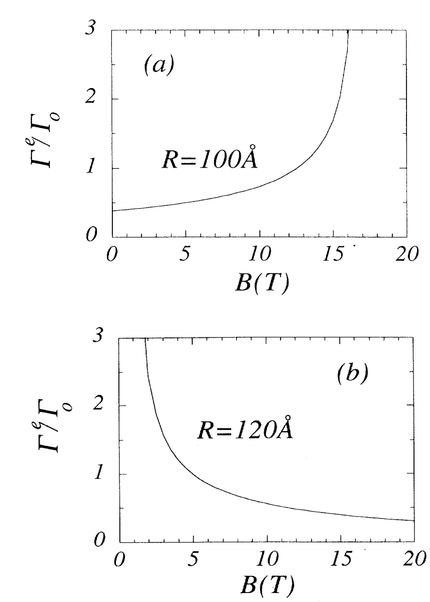

FIG. 6. The intersubband scattering rate as a function of axial field for (a) $(-1,1)$ to (0,1) transitions and (b) (1,1) to (0,1) transitions ($\varepsilon_i=0$ for both curves).

tween $(-1,1)$ and (0,1) for a 100-Å wire and Fig. 6(b) the intersubband rate between (1,1) and (0,1) for a wire radius of 120 Å as a function of axial field (for both diagrams $\varepsilon_i=0$). The divergences in both curves at the critical fields are again due to the divergent nature of the 1D density of states.

IV. DISCUSSIONS AND CONCLUSIONS

In this paper we have investigated in detail scattering rates for electrons in cylindrical wires interacting with bulk LO phonons both with and without an applied magnetic field. Analytic results were obtained by employing the approximate wave functions of Gold and Gazali and these were demonstrated to lead to an excellent agreement with the purely numerical calculations. In the presence of an axial magnetic field, interesting behavior was demonstrated for the first-order intersubband relaxation, due to the Zeeman splitting of the first excited subband. In particular, we identified two critical fields depending on whether the zero-field splitting was greater or less than the LO-phonon energy. The former depends on the decrease in energy of the $m=-1$ subband with increasing magnetic field. The latter, on the other hand, depends on the increase in energy of the $m=1$ subband with increasing axial field. This particular critical field, which for $R=120$ Å is around 1 T, is particularly amenable to experimental investigation due to the small field. In both cases it is predicted that intersubband relaxation is considerably enhanced close to the critical field. It is therefore demonstrated that the application of an axial external field to a one-dimensional system can lead the adjustment of the energy-level separations in order to achieve fast intersubband carrier relaxation. As far as we are aware, this is the first time that the application of magnetic fields in order to enhance the electron–LO-phonon interaction in 1D has been discussed.

In our analysis of the scattering rates calculated here we have made some implicit theoretical assumptions that need to be justified over and above those already mentioned in the previous sections. Our main aim was to develop an analytic approach to the description of the electron–LO-phonon interaction in cylindrical wires. This is a one-particle theory and we have ignored the effects of electron-electron interactions. The inclusion of these effects has been considered recently for cylindrical wires.[32] The main effect is the renormalization of the interaction Hamiltonian by the dielectric function (obtainable by, e.g., the random-phase approximation). For carrier concentrations of less than $10^5\ \mathrm{cm}^{-1}$ this is negligible;[33] larger concentrations and the rates are reduced *without* an appreciable change in the trends. In particular, the prediction of the divergence in the intersubband rates at the critical fields will still hold. This leads naturally to the question of the use of first-order perturbation theory when the interaction strength diverges. The relevant parameter here is α (≈ 0.078 for GaAs), the Fröhlich coupling parameter [Eq. (16)]. If the rate is a few Γ_0, then first-order perturbation theory should still be valid larger, and it is questionable. Luckily, whenever the scattering rates diverge they do so over a very narrow range and one may then be confident that the results obtained by the straightforward approach adopted here are valid, except very close to the singularity.

Finally, the Gold and Ghazali wave functions also facilitate analytic results for acoustic-phonon interactions in cylindrical wires, both deformation potential and piezoelectric scattering,[34] which will be the subject of further investigation.

Recently, Telang and Bandyopadhyay[35] and Shik and Challis[36] have reported the effect of a magnetic field on the acoustic-phonon scattering rates in quantum wires. These rates are significantly reduced when a field is applied.

ACKNOWLEDGMENTS

We would like to thank the University of Botswana (M.M.) and the United Kingdom Science and Engineering Research Council (N.C.C.) for financial support. We also acknowledge useful discussions with Professor B. K. Ridley, Professor D. R. Tilley, and Dr. B. Tanatar.

APPENDIX

In the evaluation of the infinite integral of Eq. (10) using the approximate overlap integrals of Eqs. (23) and (24) we are led to the evaluation of integrals of the form

$$W_n(Q)=\int_0^\infty \frac{J_n^2(y)}{y^5(y^2+Q^2)}dy \ . \tag{A1}$$

In principle, these may be found in Gradshteyn and Ryzhik,[31] but, as has been pointed out by Fishman,[12] these are incorrectly stated. The easiest way to evaluate the above is via the use of partial fractions, viz.,

$$\frac{1}{y^5(y^2+Q^2)}=\frac{1}{Q^6}\left[\frac{1}{y}-\frac{Q^2}{y^3}+\frac{Q^4}{y^5}-\frac{y}{y^2+Q^2}\right] \tag{A2}$$

and hence $W_n(Q)$ may now be evaluated by employing the following standard integrals which may be found in Gradshteyn and Ryzhik

$$\int_0^\infty \frac{J_n^2(y)}{y^\lambda}dy=\frac{\Gamma(\lambda)\Gamma\left[\frac{2n-\lambda+1}{2}\right]}{2^\lambda\Gamma^2\left[\frac{\lambda+1}{2}\right]\Gamma\left[\frac{2n+\lambda+1}{2}\right]} \tag{A3}$$

and

$$\int_0^\infty \frac{yJ_n^2(y)}{y^2+Q^2}dy=I_n(Q)K_n(Q) \ , \tag{A4}$$

where in (A4) $I_n(z)$ and $K_n(z)$ are modified Bessel functions.[22] The integrals required in the text are therefore

$$W_3(Q)=\frac{1}{Q^6}\left\{\frac{1}{6}-\frac{Q^2}{96}+\frac{Q^4}{640}-I_3(Q)K_3(Q)\right\} , \tag{A5}$$

$$W_4(Q)=\frac{1}{Q^6}\left\{\frac{1}{8}-\frac{Q^2}{240}+\frac{Q^4}{3840}-I_4(Q)K_4(Q)\right\} . \tag{A6}$$

*Author to whom all correspondence should be addressed.

[1]J. Cibert, P. M. Petroff, G. J. Dolan, S. J. Pearton, A. C. Gossard, and J. H. English, Appl. Phys. Lett. **49**, 1275 (1986).

[2]K. F. Berggren, T. J. Thornton, D. J. Newson, and M. Pepper, Phys. Rev. Lett. **57**, 1130 (1986).

[3]K. Ismail, D. A. Antoniades, and H. I. Smith, Appl. Phys. Lett. **54**, 1757 (1989).

[4]A. Menschig, A. Forchel, B. Roos, R. Germann, K. Pressel, W. Heuring, and D. Grutzmacher, Appl. Phys. Lett. **57**, 1757 (1990).

[5]A. S. Plaut, H. Lage, P. Grambow, D. Heitman, K. von Klitzing, and K. Ploog, Phys. Rev. Lett. **67**, 1642 (1991).

[6]H. Sasaki, Jpn. J. Appl. Phys. **19**, L735 (1980).

[7]G. Fishman, Phys. Rev. B **34**, 2394 (1986).

[8]J. P. Leburton, J. Appl. Phys. **56**, 2850 (1984).

[9]V. P. Campos and S. Das Sarma, Phys. Rev. B **45**, 3898 (1992).

[10]N. C. Constantinou and B. K. Ridley, J. Phys. Condens. Matter **1**, 2283 (1989).

[11]S. A. Leao, O. Hipolito, and F. M. Peeters, Superlatt. Microstruct. **13**, 37 (1993).

[12]G. Fishman, Phys. Rev. B **36**, 7448 (1987).

[13]A. Gold and A. Ghazali, Phys. Rev. B **41**, 7626 (1990).

[14]R. J. Tonucci, B. L. Justus, A. J. Campillo, and C. E. Ford, Science **258**, 783 (1992).

[15]S. V. Branis, G. Li, and K. K. Bajaj, Phys. Rev. B **47**, 1316 (1993).

[16]G. Ihm, M. L. Falk, S. K. Noh, S. J. Lee, and T. W. Kim, Phys. Rev. B **46**, 15 270 (1993).

[17]N. C. Constantinou, M. Masale, and D. R. Tilley, J. Phys. Condens. Matter **4**, 4499 (1992).

[18]M. Masale, N. C. Constantinou, and D. R. Tilley, Phys. Rev. B **46**, 15 432 (1993).

[19]N. Mori and T. Ando, Phys. Rev. B **40**, 6175 (1989).

[20]H. Rucker, E. Molinari, and P. Lugli, Phys. Rev. B **45**, 6747 (1992).

[21]B. K. Ridley, *Quantum Processes in Semiconductors,* 2nd ed. (Clarendon, Oxford, 1982).

[22]*Handbook of Mathematical Functions,* edited by M. Abramowitz and I. A. Stegan (Dover, New York, 1965).

[23]K. T. Tsen, K. R. Wald, T. Ruf, P. Y. Yu, and H. Morkoc, Phys. Rev. Lett. **67**, 2577 (1991).

[24]M. C. Tatham, J. F. Ryan, and C. T. Foxon, Phys. Rev. Lett. **63**, 1637 (1989).

[25]H. T. Grahn, H. Schneider, W. W. Ruhle, K. von Klitzing, and K. Ploog, Phys. Rev. Lett. **64**, 2426 (1990).

[26]G. Mayer, F. E. Prins, G. Lehr, H. Scweizer, H. Leier, B. E. Maile, and G. Weimann, Phys. Rev. B **47**, 4060 (1993).

[27]Y. Oowaki, J. E. Frost, L. Martin-Moreno, M. Pepper, D. A. Ritchie, and G. A. C. Jones, Phys. Rev. B **47**, 4088 (1993).

[28]P. J. Price, Ann. Phys. (N.Y.) **133**, 217 (1981).

[29]B. K. Ridley, J. Phys. C **15**, 5899 (1982).

[30]R. B. Dingle, Proc. R. Soc. London Ser. A **212**, 47 (1952).

[31]I. S. Gradshteyn and I. M. Ryzhik, *Table of Integrals, Series and Products* (Academic, New York, 1980), p. 679, Eq. 6.541.2.

[32]B. Tanatar, J. Phys. Condens. Matter **5**, 2203 (1993).

[33]B. Tanatar (private communication).

[34]N. C. Constantinou (unpublished).

[35]N. Telang and S. Bandyopadhyay, Appl. Phys. Lett. **62**, 3161 (1993).

[36]A. Y. Shik and L. J. Challis, Phys. Rev. B **47**, 2082 (1993).